Published as:
Krasnikov, S. A.; Doyle, C. M.; Sergeeva, N. N.; Preobrajenski, A. B.; Vinogradov, N. A.; Sergeeva, Y. N.; Zakharov, A. A.; Senge, M. O.; Cafolla, A. A. (2011):
Formation of Extended Covalently Bonded Ni Porphyrin Networks on the Au(111) Surface.
Nano Research **4**, 376–384.

The formation of extended covalently bonded Ni porphyrin networks on the Au(111) surface

Sergey A. Krasnikov, [*,1] *Catherine Doyle,* [1] *Natalia N. Sergeeva,* [2] *Alexei B. Preobrajenski,* [3] *Nikolay A. Vinogradov,* [3] *Yulia N. Sergeeva,* [2] *Alexei A. Zakharov,* [3] *Mathias O. Senge,* [2] *and Attilio A. Cafolla* [1].

School of Physical Sciences, Dublin City University, Glasnevin, Dublin 9, Ireland, SFI Tetrapyrrole Laboratory, School of Chemistry, Trinity College Dublin, Dublin 2, Ireland and MAX-lab, Lund University, Box 118, 22100 Lund, Sweden.

Sergey.Krasnikov@dcu.ie

RECEIVED DATE (to be automatically inserted after your manuscript is accepted if required according to the journal that you are submitting your paper to)

* To whom correspondence should be addressed. E-mail: Sergey.Krasnikov@dcu.ie

1 Dublin City University.

2 Trinity College Dublin.

3 MAX-lab, Lund University.

ABSTRACT The growth and ordering of {5,10,15,20-tetrakis(4-bromophenyl)porphyrinato}nickel(II) (NiTBrPP) molecules on the Au(111) surface have been investigated using scanning tunneling microscopy, x-ray absorption, core-level photoemission and microbeam low-energy electron diffraction. When deposited onto the substrate at room temperature the NiTBrPP forms a well-ordered close-packed molecular layer in which the molecules have a flat orientation with the porphyrin macrocycle plane

lying parallel to the substrate. Annealing of the NiTBrPP layer on the Au(111) surface at 525 K leads to dissociation of bromine from the porphyrin followed by the formation of covalent bonds between the phenyl substituents of the porphyrin. This results in the formation of large covalently bonded porphyrin networks, which are stable up to 800 K and can be recovered after exposure to ambient conditions. By controlling the experimental conditions a robust, extended porphyrin network can be prepared on the Au(111) surface that has many potential applications including protective coatings, sensing or as a host structure for molecules and clusters.

Introduction. Molecular self-assembly may be defined as the spontaneous association of molecules under equilibrium conditions into stable, structurally well defined aggregates mediated by non-covalent bonds.[1-3] The basic idea is to utilize molecular building blocks with predetermined intermolecular bonding properties. However, since molecular self-assembly is based on non-covalent interactions (e.g., hydrogen bonding, metal ligand bonding or van der Waals interactions),[4-13] the stabilization energies are usually very low. As a consequence conventional self-assembled structures are often unstable even at moderate temperatures. A strategy to overcome this low stabilization energy relies on inducing covalent reactions between the molecular components, thus forming two-dimensional covalently bonded networks. The formation of covalent bonds between complementary molecular components is an appealing approach in the fabrication of nanoscale structures, such as nanomeshes and nanolines, because of their high selectivity, strength and directionality.[3,14-26] These nanostructures are attractive both for their intrinsic properties; for their potential applications such as novel sensing, energy conversion or catalytic devices; for their ability to 'trap' other molecules such as fullerenes, creating even more interesting complexes and for their use as templates to direct the growth of, for example, metal clusters with interesting catalytic or magnetic properties.

Although covalently bonded systems in general show much higher stabilities, their coordination is more difficult to control and the bonding is irreversible. Despite their potential high technological impact, surface supported covalently bonded networks have attracted increasing attention only recently. These covalent systems include polycondensation reactions of imides[15,16] and imines,[17,18] periodically

corrugated monolayers of boron nitride[19-22] and graphene,[23,24] networks based on boronate chemistry,[25] and, recently, the first example of a two-dimensional surface supported porphyrin network with domain sizes of ~10nm.[14] The characteristic or repeat dimensions of these molecular networks are typically in the range of 5 to 20 nm, at a length scale where conventional lithographic techniques are no longer applicable. Although these nanomeshes are thermally less stable than traditional inorganic zeolites, they exhibit an enormous chemical and structural versatility, because they are built from easily modifiable molecular building blocks. Several nanomeshes capable of hosting guest molecules have been reported,[26,27] and host–guest interactions have been investigated, for example, through temperature-controlled desorption studies of the accommodated guest molecules.[27] The study of these surface-supported systems is important for future developments in molecular electronics, since they represent promising materials for applications in nanopatterning, surface templating, molecular data storage, quantum computing, sensors/molecular recognition, highly selective catalysis and functional/biomimetic surfaces.[26-30]

Functionalized porphyrin derivatives[31] are excellent candidates as the basic building blocks for covalently bonded networks. Porphyrins have attracted considerable attention because they are utilized in an ever-expanding array of applications ranging from molecular optoelectronic gates, molecular wires, photo-inducible energy or electron transfer systems, light-harvesting arrays for solar energy generation, enzyme models, oxidation catalysts, nonlinear optics and photodynamic therapy.[30-33] Porphyrin molecules with extended π-electron systems have found wide use in the construction of potential molecular devices because they tend to bond to surfaces in a flat-lying geometry, which allows functional groups at the molecular periphery to approach each other easily and to engage in bonding interactions. Recently, a rich variety of molecular nanostructures such as clusters, wires and extended networks have been prepared on different surfaces using porphyrin derivatives and characterized by scanning tunneling microscopy.[2-4,8-12,14,26,34-36]

In the present work we focus on the formation of covalently bonded Ni porphyrin networks on the Au(111) surface by using scanning tunneling microscopy (STM), near-edge x-ray absorption fine

structure (NEXAFS) and core-level photoemission spectroscopy (XPS). These networks are constructed from the {5,10,15,20-tetrakis(4-bromophenyl)porphyrinato}nickel(II) building blocks via thermally-controlled dissociation of bromine from the porphyrin. The results of this work yield important information about the electronic and structural properties, temperature stability and contamination resistance of porphyrin networks.

Experimental Details. The STM experiments were performed at room temperature, using a commercial instrument (Omicron Nanotechnology GmbH), in an ultra-high-vacuum (UHV) system consisting of an analysis chamber (with a base pressure of 2×10^{-11} mbar) and a preparation chamber (8×10^{-11} mbar) connected to the main chamber through a gate valve. An electrochemically etched polycrystalline tungsten tip was used to record STM images in constant current mode. The voltage V_{sample} corresponds to the sample bias with respect to the tip. No drift corrections have been applied to any of the STM images presented in this paper. A single-crystal Au(111) surface (Surface Preparation Laboratory) was used as a substrate. The Au(111) crystal was cleaned *in situ* by repeated cycles of argon ion sputtering at 1 kV and annealing at 870 K for 20 minutes until a LEED pattern with sharp diffraction spots was obtained.

The NiTBrPP was synthesized according to a published procedure.[14] The NiTBrPP was evaporated in a preparation chamber isolated from the STM chamber at a rate of about 0.1 ML (monolayer) per minute from a tantalum crucible in a homemade deposition cell operated at a temperature of approximately 600 K. The total pressure during porphyrin deposition was in the 10^{-10} mbar range. Before evaporation the NiTBrPP powder was degassed at approximately 500 K for about 10 hours to remove water vapor.

All spectroscopic measurements were performed at beamline D1011, MAX-lab, Lund University. XPS spectra were measured with a Scienta SES-200 electron energy analyzer. The kinetic energy resolution was set to 75 meV for the N 1s and Br 3d spectra. The photon energy resolution was set to 70 meV at the C K-edge (~280 eV), to 100 meV at the N K-edge (~400 eV) and to 200 meV at the Ni L_3-edge (~850 eV). The base pressure during the measurements did not exceed 2×10^{-10} mbar. The

NEXAFS spectra were recorded in the partial electron yield mode (with a bias of -100 V) using a multichannel plate detector and normalized to the background curves recorded from the clean substrate. Low energy electron microscopy and micro-diffraction were performed with Elmitec LEEM III microscope at beamline I311, MAX-lab, Lund University.

Results and Discussion. Ni porphyrins represent a class of flexible molecules with a nearly square planar core conformation.[30,33] The molecular structure of the {5,10,15,20-tetrakis(4-bromophenyl)porphyrinato}nickel(II) is shown in Figure 1a. If deposited onto the substrate at room temperature the NiTBrPP self-assembles on the Au(111) surface forming large well-ordered molecular domains (approximately 100 nm × 100 nm) with a close-packed square structure. Figure 1b shows typical occupied state STM images of a single domain taken from 1 ML of the NiTBrPP on the Au(111) surface. In the NiTBrPP overlayer the macrocycle (the central Ni atom surrounded by four pyrrole rings) of each molecule has a flat orientation on the surface with the molecular plane lying parallel to the substrate. The macrocycle of the molecule has a four-fold D_{4h} symmetry and appears as four lobes in Figure 1b. However, some of the molecules show two lobes which appear in one of two orthogonal orientations. The presence of two lobes indicates that the expected four-fold symmetry is broken for these molecules. This is attributed to a distortion of the macrocycle into a 'saddle' conformation on the substrate where two opposing pyrrole rings in the macrocycle bend away from the substrate.[36-39]

A flat orientation of the porphyrin macrocycle on the Au(111) surface was further confirmed by angular dependent N 1s NEXAFS spectra (not shown here). The unit cell of the NiTBrPP lattice (shown in black in Figure 1b) contains a single NiTBrPP molecule and has the following parameters: the unit cell vectors are equal to 1.60 ± 0.05 nm, while the angle between them is 90.0º ± 0.5º, forming a square close packed structure. The formation of ordered domains of such extent indicates the presence of a strong intermolecular interaction as well as a low diffusion barrier for the molecules on this surface at room temperature. In turn, a microbeam LEED pattern acquired from a sample area of 1.5 μm^2 (see Figure 1, inset) shows the presence of multiple domains on the surface indicating a weak molecule-substrate interaction which is usual for low reactivity substrates such as Au. Thus, NiTBrPP molecules

are physisorbed on the Au(111) surface and a weak molecule-substrate interaction occurs through the molecular π-electron system.

All STM images of the NiTBrPP molecules deposited on the Au(111) surface at room temperature show a close-packed structure of the self-assembled layer with a small separation between the molecules. This is a result of significant rotation of the phenyl rings attached to the porphyrin macrocycle. The plane of the phenyl rings is usually rotated by 50º - 60º with respect to the macrocycle plane according to *ab initio* calculations, STM and x-ray absorption experiments.[36-39] Such rotation allows the NiTBrPP molecules to approach each other on the surface in a well defined manner when intermolecular bonding occurs through the π-electron system of the phenyl rings (π-π bonding) as well as through Br ··· H–C hydrogen bonds.

Annealing of the NiTBrPP layer on the Au(111) surface at 525 K leads to a striking change in the structure of the molecular overlayer. Figure 2 shows changes in the Br 3d core-level XPS as a result of the substrate anneal. The Br 3d signal starts to decrease at a substrate temperature of 370 K and disappears completely after annealing the system at 525 K for 30 min. Annealing to these temperatures results in dissociation of bromine from the phenyl rings. This process is followed by a formation of covalent bonds between phenyl rings linking porphyrin molecules to each other. Comparatively weak carbon–halogen bonds are well suited as predetermined breaking points to assist in the formation of covalently bonded networks on surfaces.[14,40] The homolytic bond dissociation energy of C–Br bonds (3.2 eV)[41] is substantially lower than that of the C–C link between phenyl rings (4.8 eV)[42] making such a reaction possible on surfaces at a relatively low temperature.

The quality of covalently bonded Ni(II) 5,10,15,20-tetraphenylporphyrin (NiTPP) networks depends on the preparation conditions. Figure 3 shows typical STM images taken after the deposition of a NiTBrPP layer onto the Au(111) surface at room temperature and subsequent annealing to form NiTPP organic networks. The 22 × √3 herringbone reconstruction of the underlying Au(111) substrate is also visible (Figure 3c). After annealing of the initially deposited 1.5 ML of the NiTBrPP, the porphyrin molecules form continuous networks which extend over the entire substrate (Figure 3a). Topological

defects such as five-membered rings, porphyrins bonding in incorrect configurations and adjacent phenyl rings failing to bond are observed in the networks (Figure 3). These networks also include regions of perfectly coordinated nanomesh with a pore size of 1.1 nm where each porphyrin is bonded to four neighboring molecules. The average size of these regions is typically 10 nm × 10 nm (Figures 3a and 3c). The disorder within the porphyrin network may be attributed to the preparation procedure which involves annealing an initially self assembled close packed NiTBrPP monolayer (Figure 1b). In this case, such a dense packing results in a restricted movement of the molecules during annealing, thus preventing the necessary expansion of the molecular layer which is required for perfect nanomesh formation. In the latter the distance between adjacent molecules is 1.8 nm (Figure 3c) which is larger by 13% than the 1.6 nm molecule-molecule separation in the self-assembled layer (Figure 1b). Furthermore, nanomesh nucleation can occur between any pair of molecules resulting in a large number of nucleation sites. Once nucleation is initiated at a given point this will dictate the local orientation of the nanomesh forcing other molecules to adjust their position. The lack of space limits this adjustment leading to the observed defects in the network. When the initial coverage of the NiTBrPP is lower than one monolayer (0.3 – 0.8 ML) the annealing procedure does not produce networks of improved quality (Figure 3c). This is due to the fact that at low coverage the NiTBrPP molecules still form compact self-assembled islands because of the weak molecule-substrate interaction.

In an attempt to improve the quality of the porphyrin networks they were also prepared by depositing the molecules onto the Au(111) surface held at an elevated temperature of 475 K. In this case the bromine dissociates from the phenyl rings on contact with the surface. The sticking coefficient of the molecules on the surface is reduced by the increased temperature, which leads to lower network coverage for an equivalent molecular dose. Figure 4 shows typical STM images from the NiTBrPP layer formed on a surface at elevated temperature. It is clear that in this case the porphyrin networks tend to grow from the step-edges (Figure 4a) which provides additional evidence for a weak molecule-substrate interaction and for the diffusion of the molecules on the Au(111) surface. Significantly, the areas of

ideal nanomesh are comparable in size with the previous method of formation, indicating that mesh size is not dependent on the procedure, but rather is limited by the defect density of the network.

Figure 5 shows C 1s NEXAFS spectra obtained from the NiTBrPP layer on the Au(111) surface at different stages during preparation of the network. The angle between the polarization vector of incoming synchrotron radiation and the substrate surface normal was 45°. The spectra in Figure 5 are very similar, confirming that the molecules remain intact during the anneal. The spectrum measured from the 1.5 ML of the NiTBrPP on the Au(111) surface shows two sharp low-energy π resonances at 284.8 eV and 285.7 eV denoted in Figure 5 by A and B, respectively. Based on the comparative analysis of NEXAFS spectra measured from (porphyrinato)nickel(II) and {5,10,15,20-tetraphenylporphyrinato}nickel(II), it was found that the absorption structure A is associated with transitions of C 1s electrons to hybridized Ni 3dπ - ligand (C and N) 2pπ unoccupied states localised within the porphyrin macrocycle.[43,44] In turn, the major contribution to the absorption structure B is due to transitions of C 1s electrons to C 2pπ unoccupied states localised within the phenyl rings of the porphyrin.[43,44]

There are two main changes observed in the C 1s spectra due to annealing of the NiTBrPP layer on the Au(111) surface: (i) a decrease of intensity of the peak B and (ii) an overall broadening of the π resonances A-D. The first finding can be attributed to the additional rotation of phenyl rings relative to the porphyrin macrocycle due to the formation of C-C bonds between the phenyl rings of adjacent molecules upon annealing. As a result of such a covalent bonding the phenyl rings align almost perpendicular to the macrocycle (and the Au(111) surface), which can be seen in STM images shown in Figures 3 and 4. This change in the angle between the polarization vector of incoming photons and the surface normal of the phenyl rings leads to a decrease in intensity of the corresponding π resonance (peak B), which depends strongly on the polarization of the incident photons.[45,46] In turn, an overall broadening of the π resonances A-D is associated with the formation of a large macromolecule (that is the covalently bonded NiTPP network) with a π-conjugated electron system. The π-conjugation leads to

a significant delocalization of the π electron states, which results in a broadening of the corresponding π resonances in NEXAFS spectra.

The networks have proven to be extremely stable with respect to both temperature and exposure to ambient conditions. Figure 6a shows an STM image of a network recorded after it was removed from the vacuum system and exposed to ambient conditions for 60 hours. After exposure the surface was difficult to image and clearly showed adsorbed material, however there is evidence that the network persists on the surface underneath this contaminating layer. This surface was subsequently annealed to 675 K for 30 minutes resulting in the complete removal of the adsorbed material and recovery of the network on the surface (see Figure 6b). To study the thermal stability of the network, the system was further annealed to 775 K. STM images taken after this treatment (Figure 6c) show that the network remains intact on the surface. The molecules can be resolved clearly and appear identical to those recorded in Figure 3. The procedures described in this work provide a simple, two-step method for the preparation of porphyrin functionalized surfaces which are both thermally and mechanically stable. Such stability offers many advantages for potential applications such as protective coatings, gas sensing, photovoltaic devices and nanostructured templates suitable for hosting other molecules.

Conclusions. The growth and ordering of NiTBrPP molecules on the Au(111) surface have been investigated using STM, NEXAFS and XPS. Results indicate that at room temperature the NiTBrPP forms a well-ordered close-packed molecular layer on the Au(111) in which the porphyrin molecules have a flat orientation with the macrocycle plane lying parallel to the substrate. Annealing of the NiTBrPP layer on the Au(111) surface at 525 K leads to a complete dissociation of bromine from the porphyrin followed by the formation of covalent bonds (C-C) between the phenyl rings of the porphyrin. This results in the formation of continuous covalently bonded NiTPP networks, which extend over the entire substrate. Such a NiTPP network represents a large macromolecule with a π-conjugated electron system. The results presented demonstrate that this porphyrin system is stable up to 800 K and can be regenerated after exposure to ambient conditions. Molecular networks with such

properties can be exploited in a range of novel applications and provide a starting point for the construction of more complex molecular nanostructures and electronic devices.

Acknowledgement. This work was supported by the Irish Higher Education Authority PRTLI programme and by Science Foundation Ireland through the Research Frontiers Programme (grant number 08/RFP/PHY1366) and a Principal Investigator grant (SFI P.I. 09/IN.1/B2650). C.M.D. gratefully acknowledges the Irish Research Council for Science, Engineering and Technology, funded by the National Development Plan. Y.N.S. gratefully acknowledges a Science Foundation Ireland UREKA 2008 award. STM topographic images were processed using WSxM software.[47]

FIGURE CAPTIONS

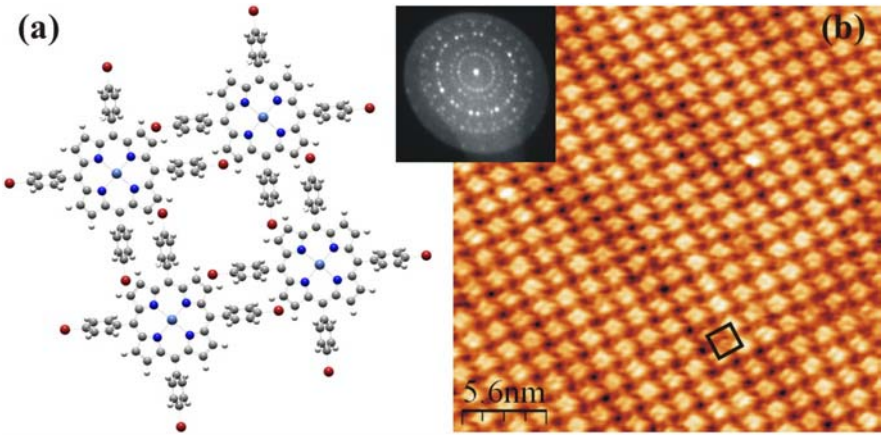

Figure 1. (a) Molecular model of four self-assembled NiTBrPP molecules. (b) STM image of 1 ML of the NiTBrPP self-assembled on the Au(111) surface, V_{sample} = -1.4 V, I_t = 0.7 nA, size 28 nm × 28 nm. The unit cell of the NiTBrPP lattice is shown in black (b) and has the following parameters: the unit cell vectors are equal to 1.60 nm ± 0.05 nm, and the angle between them is 90.0º ± 0.5º. Inset shows a microbeam LEED pattern for 1 ML of the NiTBrPP on the Au(111) acquired at a primary beam energy of 11.5 eV. The sampling area for microbeam LEED was 1.5 μm^2.

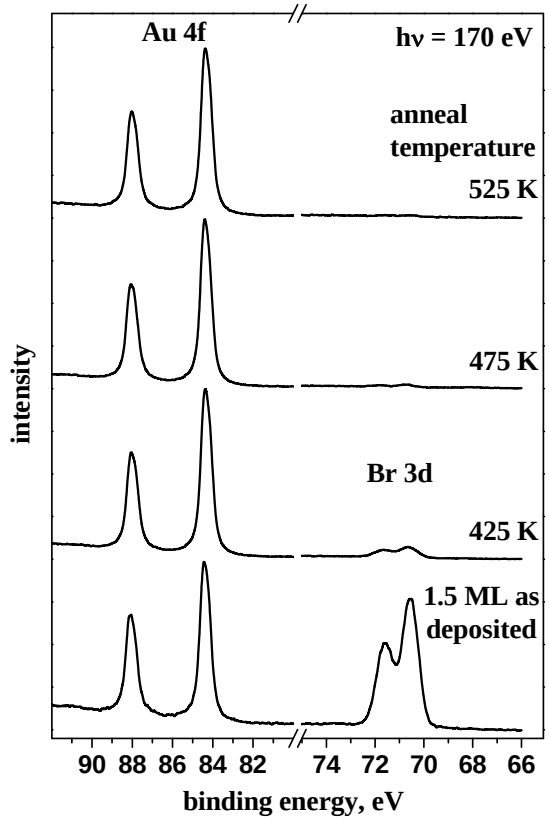

Figure 2. Au 4f and Br 3d core-level XPS spectra measured from the Ni porphyrin layer on the Au(111) surface after annealing the system at different temperatures. Excitation energy is equal to 170 eV.

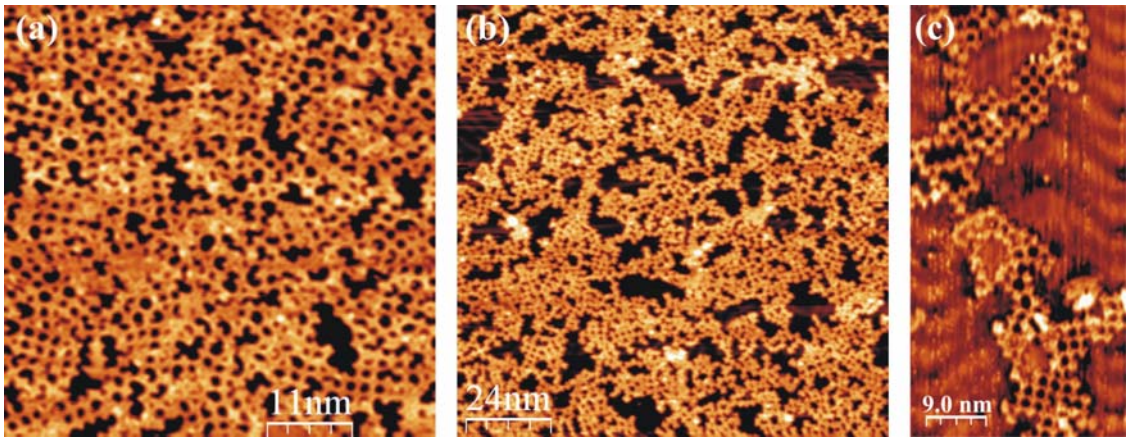

Figure 3. STM images of covalently bonded NiTPP networks on the Au(111) surface, formed by room temperature deposition followed by annealing. (a) 1.5 ML annealed at 445 K, V_{sample} = +1.0 V, I_t = 1.0 nA, size 54 nm × 54 nm. (b) 1 ML annealed at 575 K, V_{sample} = -1.25 V, I_t = 0.35 nA, size 120 nm × 120 nm. (c) 0.3 ML annealed at 525 K, V_{sample} = +1.25 V, I_t = 0.15 nA, size 30 nm × 60 nm.

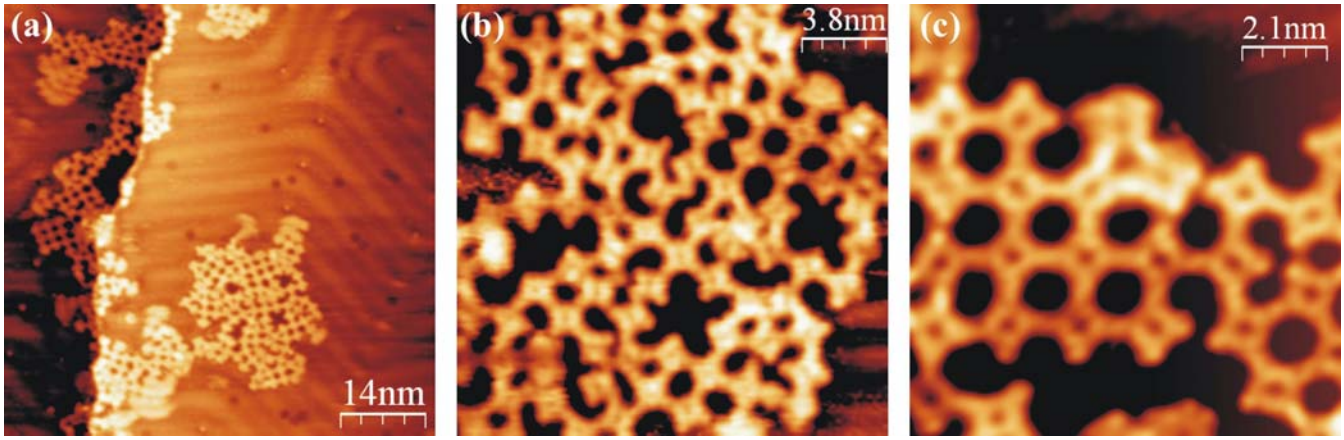

Figure 4. STM images of covalently bonded NiTPP networks formed on the Au(111) surface by molecular deposition onto the substrate at an elevated temperature of 475 K. (a) V_{sample} = +1.4 V, I_t = 0.6 nA, size 70 nm × 70 nm. (b) V_{sample} = +1.4 V, I_t = 0.6 nA, size 19 nm × 19 nm. (c) V_{sample} = -0.75 V, I_t = 0.65 nA, size 11 nm × 11 nm.

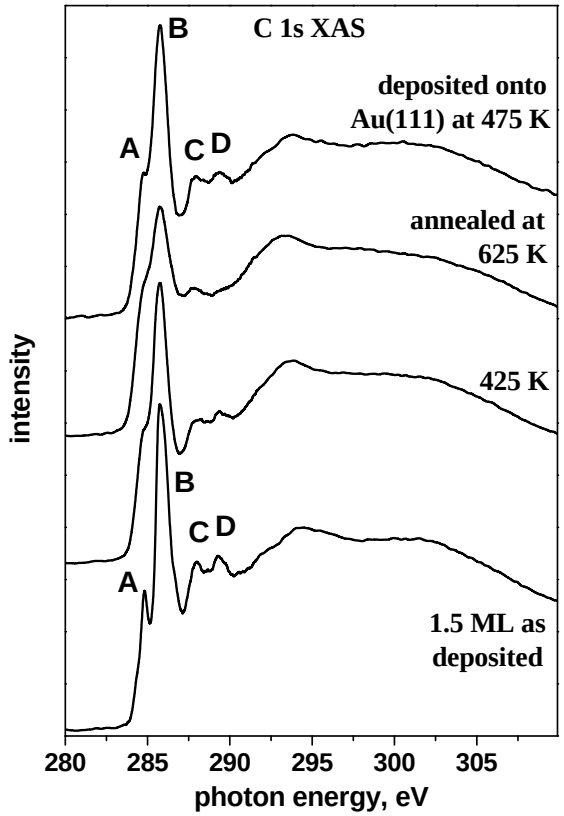

Figure 5. C 1s NEXAFS spectra measured from the Ni porphyrin layer on the Au(111) surface for different preparation conditions. The three lower spectra were recorded after deposition at room temperature (bottom spectrum) and subsequent annealing. Top spectrum was recorded after deposition onto a hot substrate at 475 K.

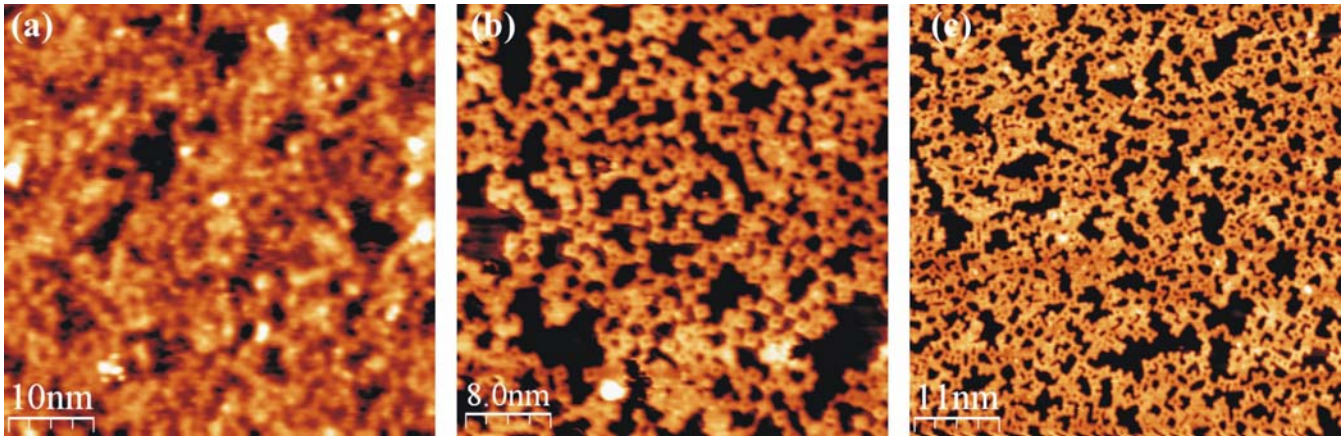

Figure 6. STM images of covalently bonded NiTPP networks on the Au(111) surface. (a) After exposure to ambient conditions for 60 hours, V_{sample} = +1.0 V, I_t = 0.5 nA, size 50 nm × 50 nm. (b) Sample in (a) annealed at 675 K, V_{sample} = +1.0 V, I_t = 1.0 nA, size 40 nm × 40 nm. (c) After annealing at 775 K, V_{sample} = +0.6 V, I_t = 1.5 nA, size 55 nm × 55 nm.

REFERENCES

(1) Whitesides, G. M.; Mathias, J. P.; Seto, C. T. *Science* **1991**, *254*, 1312.

(2) Barth, J. V.; Costantini, G.; Kern, K. *Nature* **2005**, *437*, 671.

(3) Barth, J. V. *Ann. Rev. Phys. Chem.* **2007**, *58*, 375.

(4) Elemans, J. A. W.; van Hameren, R.; Nolte, R. J. M.; Rowan, A. E. *Adv. Mater.* **2006**, *18*, 1251.

(5) Whitesides, G. M.; Grzybowski, B. *Science* **2002**, *295*, 2418.

(6) Pawin, G.; Wong, K. L.; Kwon, K.-Y.; Bartels, L. *Science* **2006**, *313*, 961.

(7) Ikkala, O.; ten-Brinke, G. *Science* **2002**, *295*, 2407.

(8) van Hameren, R.; Schon, P.; van Buul, A. M.; Hoogboom, J.; Lazarenko, S. V.; Gerritsen, J. W.; Engelkamp, H.; Christianen, P. C. M.; Heus, H. A.; Maan, J. C.; Rasing, T.; Speller, S.; Rowan, A. E.; Elemans, J. A. W.; Nolte, R. J. M. *Science* **2006**, *314*, 1433.

(9) Yanagi, H.; Mukai, H.; Ikuta, K.; Shibutani, T.; Kamikado, T.; Yokoyama, S.; Mashiko, S. *Nano Lett.* **2002**, *2*, 601.

(10) Eichberger, M.; Marschall, M.; Reichert, J.; Weber-Bargioni, A.; Auwärter, W.; Wang, R. L. C.; Kreuzer, H. J., Pennec, Y.; Schiffrin, A.; Barth, J. V. *Nano Lett.* **2008**, *8*, 4608.

(11) Heim, D.; Seufert, K.; Auwärter, W.; Aurisicchio, C.; Fabbro, C.; Bonifazi, D.; Barth, J. V. *Nano Lett.* **2009**, *10*, 122.

(12) Krasnikov, S. A.; Beggan, J. P.; Sergeeva, N. N.; Senge, M. O.; Cafolla, A. A. *Nanotechnology* **2009**, *20*, 135301.

(13) Krasnikov, S. A.; Hanson, C. J., Brougham, D. F.; Cafolla, A. A. *J. Phys.: Condens. Matter* **2007**, *19*, 446005.

(14) Grill, L.; Dyer, M.; Lafferentz, L.; Persson, M.; Peters, M. V.; Hecht, S. *Nat. Nanotech.* **2007**, *2*, 687.

(15) Bitzer, T.; Richardson, N. V. *Appl. Phys. Lett.* **1997**, *71*, 1890.

(16) Treier, M.; Richardson, N. V.; Fasel, R. *J. Am. Chem. Soc.* **2008**, *130*, 14054.

(17) Weigelt, S.; Busse, C.; Bombis, C.; Knudsen, M. M.; Gothelf, K. V.; Strunskus, T.; Wöll, C.; Dahlbom, M.; Hammer, B.; Lægsgaard, E.; Besenbacher, F.; Linderoth, T. R. *Angew. Chem. Int. Ed.* **2007**, *46*, 9227.

(18) Weigelt, S.; Busse, C.; Bombis, C.; Knudsen, M. M.; Gothelf, K. V.; Lægsgaard, E.; Besenbacher, F.; Linderoth, T. R. *Angew. Chem. Int. Ed.* **2008**, *47*, 4406.

(19) Corso, M.; Auwärter, W.; Muntwiler, M.; Tamai, A.; Greber, T.; Osterwalder, J. *Science* **2004**, *303*, 217.

(20) Berner, S.; Corso, M.; Widmer, R.; Groening, O.; Laskowski, R.; Blaha, P.; Schwarz, K.; Goriachko, A.; Over, H.; Gsell, S.; Schreck, M.; Sachdev, H.; Greber, T.; Osterwalder, J. *Angew. Chem. Int. Ed.* **2007**, *46*, 5115.

(21) Preobrajenski, A. B.; Nesterov, M. A.; Ng, M. L.; Vinogradov, A. S.; Mårtensson, N. *Chem. Phys. Lett.* **2007**, *446*, 119.

(22) Preobrajenski, A. B.; Krasnikov, S. A.; Vinogradov, A. S.; Ng, M. L.; Käämbre, T.; Cafolla, A. A.; Mårtensson, N. *Phys. Rev. B* **2008**, *77*, 085421.

(23) N'Diaye A. T.; Bleikamp, S.; Feibelman, P. J.; Michely, T. *Phys. Rev. Lett.* **2006**, *97*, 215501.

(24) Preobrajenski, A. B.; Ng, M. L.; Vinogradov, A. S.; Mårtensson, N. *Phys. Rev. B* **2008**, *78*, 073401.

(25) Zwaneveld, N. A. A.; Pawlak, R.; Abel, M.; Catalin, D.; Gigmes, D.; Bertin, D.; Porte, L. *J. Am. Chem. Soc.* **2008**, *130*, 6678.

(26) Stepanow, S.; Lingenfelder, M.; Dmitriev, A.; Spillmann, H.; Delvigne, E.; Lin, N.; Deng, X.; Cai, C.; Barth, J. V.; Kern, K. *Nature Materials* **2004**, *3*, 229.

(27) Kiebele, A.; Bonifazi, D.; Cheng, F.; Stöhr, M.; Diederich, F.; Spillmann, A. *Chem. Phys. Chem.* **2006**, *7***,** 1462.

(28) Chen, J.; Reed, M. A.; Rawlett, A. M.; Tour, J. M. *Science* **1999**, *286*, 1550,

(29) Tsuda, A.; Osuka, A. *Science* **2001**, *293*, 7.

(30) Senge, M. O.; Fazekas, M.; Notaras, E. G. A.; Blau, W. J.; Zawadzka, M.; Locos, O. B.; Mhuircheartaigh, E. M. N. *Adv. Mater.* **2007**, *19*, 2737.

(31) Senge, M. O.; Shaker, Y. M.; Pintea, M.; Ryppa, C.; Hatscher, S. S.; Ryan, A.; Sergeeva, Y. *Eur. J. Org. Chem.* **2010**, 237.

(32) Lin, V. S. Y.; DiMagno, S. G.; Therien, M. J. *Science* **1994**, *264*, 1105.

(33) Sergeeva, N. N.; Senge, M. O. In *Handbook of Porphyrin Science*; Kadish, K. M.; Smith, K. M.; Guilard, R., eds.; Vol. 3, World Scientific: Singapore, 2010, p. 325.

(34) Beggan, J. P.; Krasnikov, S. A.; Sergeeva, N. N.; Senge, M. O.; Cafolla, A. A. *J. Phys.: Condens. Matter* **2008**, *20*, 015003.

(35) Nikiforov, M. P.; Zerweck, U.; Milde, M.; Loppacher, C.; Park, T.-H.; Uyeda, H. T.; Therien, M. J.; Eng, L.; Bonnell, D. *Nano Lett.* **2008**, *8*, 110.

(36) Krasnikov, S. A.; Sergeeva, N. N.; Sergeeva, Y. N.; Senge, M. O.; Cafolla, A. A. *Phys. Chem. Chem. Phys.* **2010**, *12*, 6666.

(37) Yokoyama, T.; Yokoyama, S.; Kamikado, T.; Mashiko, S. *J. Chem. Phys.* **2001**, *115*, 3814.

(38) de Jong, M. P.; Friedlein, R.; Sorensen, S. L.; Öhrwall, G.; Osikowicz, W.; Tengsted, C.; Jönsson, S. K. M.; Fahlman, M.; Salaneck, W. R. *Phys. Rev. B* **2005**, *72*, 035448.

(39) Auwärter, W.; Weber-Bargioni, A.; Riemann, A.; Schiffrin, A.; Gröning, O.; Fasel, R.; Barth, J. V. *J. Chem. Phys.* **2006**, *124*, 194708.

(40) Gutzler, R.; Walch, H.; Eder, G.; Kloft, S.; Heckl, W. M.; Lackinger, M. *Chem. Commun.* **2009**, 4456.

(41) Kominar, R. J.; Krech, M. J.; Price, S. J. W. *Can. J. Chem.* **1978**, *56*, 1589.

(42) Szwarc, M. *Nature* **1948**, *161*, 890.

(43) Krasnikov, S. A.; Preobrajenski, A. B.; Sergeeva, N. N.; Brzhezinskaya, M. M.; Nesterov, M. A.; Cafolla, A. A.; Senge, M. O.; Vinogradov, A. S. *Chem. Phys.* **2007**, *332*, 318.

(44) Krasnikov, S. A.; Sergeeva, N. N.; Brzhezinskaya, M. M.; Preobrajenski, A. B.; Sergeeva, Y. N.; Vinogradov, N. A.; Cafolla, A. A.; Senge, M. O.; Vinogradov, A. S. *J. Phys.: Condens. Matter* **2008**, *20*, 235207.

(45) Chen, J. G. *Surf. Sci. Rep.* **1997**, *30*, 1.

(46) Ng, M. L.; Preobrajenski, A. B.; Zakharov, A. A.; Vinogradov, A. S.; Krasnikov, S. A.; Cafolla, A. A.; Mårtensson, N. *Phys. Rev. B* **2010**, *81*, 115449.

(47) Horcas, I.; Fernández, R.; Gómez-Rodríguez, J. M.; Colchero, J.; Gómez-Herrero, J.; Baro, A. M. *Rev. Sci. Instrum.* **2007**, *78*, 013705.

SYNOPSIS TOC (Word Style "SN_Synopsis_TOC"). If you are submitting your paper to a journal that requires a synopsis graphic and/or synopsis paragraph, see the Guide, Notes, Notice, or Instructions for Authors that appear in each publication's first issue of the year and the journal's homepage for a description of what needs to be provided and for the size requirements of the artwork.